



Increased identification rate of scrap metal using Laser Induced Breakdown Spectroscopy Echelle spectra[☆]



S. Merk^{a,*}, C. Scholz^a, S. Florek^b, D. Mory^a

^a *LTB Lasertechnik Berlin GmbH, Am Studio 2c, 12489 Berlin, Germany*

^b *ISAS Berlin–Leibniz-Institut für Analytische Wissenschaften ISAS e.V., Germany*

ARTICLE INFO

Article history:

Received 22 January 2015

Accepted 28 July 2015

Available online 5 August 2015

Keywords:

LIBS
Echelle
Classification
Chemometrics
Industrial application

ABSTRACT

In this paper we address the application of an Echelle spectrometer for metal sorting tasks using laser induced breakdown spectroscopy in the industrial environment. Echelle spectrometers guarantee the simultaneous detection of broad spectral intervals with sufficient spectral resolution, which is highly desirable for LIBS applications. Until today, this benefit was overshadowed by the reduced speed of detection which typically could not exceed 10 frames per second. In this paper we present a newly developed high speed classification setup for scrap metal sorting, equipped with an Echelle spectrometer, capable of classifying 25 samples per second using a single burst double pulse excitation, a fast EMCCD camera and an externally triggered, chopper based timing. Different multivariate discriminatory techniques (PCA, PLS-DA) are applied and compared to gain maximum use of the spectra created by this setup. A simultaneous discrimination of 10 classes was done with >90% correctness for most classes and an analysis of possible sources of error unique for non-laboratory experiments is presented.

© 2015 Elsevier B.V. All rights reserved.

1. Introduction

Laser induced breakdown spectroscopy (LIBS) is a well-known analytical tool with one of the major strengths being its speed. Therefore it is a method of choice in high throughput applications where a large number of individual analytical information is required within a short time [1–4]. Sorting of scrap metal is such an application. In a typical recycling situation, pieces of scrap metal are being shred and afterwards sorted by their elemental content. The composition of the material to be sorted varies widely and every single piece needs to be analyzed individually.

As LIBS does not require (almost) any sample preparation and is capable of performing contact less analysis [5], it is a promising candidate for such an application. Several applications of applying LIBS to sorting or generally speaking classification tasks have been reported in the literature already [3,6–12]. Due to the requirement of high sample throughput, detection speed is the limiting factor in most cases. Therefore, up to now mainly Paschen–Runge or Czerny–Turner spectrometers coupled with photomultiplier tubes or linear CCD detectors are being widely used [4,13].

Echelle spectrometers seem to be particularly suitable for LIBS applications due to their high spectral resolution, the broad simultaneously

detectable wavelength range and the compact setup. But the two dimensional character of the Echelle spectrum pattern requires, particularly for high-speed sorting, a fast and sensitive 2D-array detector. Normally ICCD-cameras which provide the required time resolution to separate the specific atomic emission from the unspecific Bremsstrahlung are used as detectors for LIBS Echelle spectrometers. But compared to state-of-the-art back-thinned CCD and EMCCD detectors these cameras are typically expensive, big and are affected by lower spatial resolution and reduced quantum efficiency of the image intensifier photocathodes.

The development of fast and inexpensive 2D EMCCD cameras [14] has allowed us to build the first high speed sorting setup based on remote LIBS detection by an Echelle spectrograph. The necessary time resolution is realized by a fast rotating chopper wheel [15] in front of the entrance slit. In the application shown in this paper the chopper is synchronized with the experimental setup and the conveyor belt as an external trigger source. Contrary to ICCD cameras, in this way the full spatial resolution and the high UV quantum efficiency of the CCD detector can be used for high performance spectrum recording [15,16]. Such a system has a very high versatility for performing different, even varying, sorting tasks which is the first key point of the present work.

To make use of the large number of spectral information covered by an Echelle spectrum, multivariate data analysis can be applied. Several chemometric methods for discriminant analysis of LIBS spectra have been shown in the literature [11,17–19]. As speed is an issue in sorting applications, algorithms need to be evaluated not only by their classification correctness but also by the time needed to apply them to new

[☆] Selected papers presented at the 8th International Conference on Laser-Induced Breakdown Spectroscopy (LIBS) in Beijing, China, 8th–12th September, 2014.

* Corresponding author. Tel.: +49 30 912075308.

E-mail address: sven.merk@ltb-berlin.de (S. Merk).

unknown samples. In the final application of the system, most of the time will be consumed by the camera readout and only little time is left for data treatment. Due to this speed issue, we have limited ourselves to the simple chemometric methods principle components analysis (PCA) and partial least squares regression discriminant analysis (PLS-DA). The other key point of this work is the comparison of a discrimination based on both techniques when applied to unknown samples.

2. Theoretical

2.1. Classification by PCA and PLS-DA

Details on PCA and PLS-DA algorithms can be found in the literature [11,20–22] and will not be repeated here. In this paper we only want to pinpoint the major differences of both techniques that influence the results presented in this work. While PCA is an unsupervised method, PLS-DA is a supervised one. This means, that during training, PCA finds the major differences in the measured spectra, represented by the principal components. However, the spectral features found by this approach do not necessarily contain any information useful for the application of interest. This may effectively result in a grouping of spectra according to other than the required properties. Such a possible grouping failure requires a good validation process in order to detect potential systematic misclassification in the later application. On the contrary, PLS-DA takes in advance the expected grouping as an input and tries to find only those features, called factors, (e.g. emission lines) useful for the requested task. Still, the classification quality should be evaluated by validation.

The typical validation approach for both techniques is cross validation [23,24]. For cross validation, some of the training spectra are left out during model building and later classified with the model created using the remaining spectra. This process is repeated several times, always taking other spectra for the validation set, and classification errors are estimated. Another validation approach is to create a separate validation set of spectra that is not included in the modeling set. This approach can be applied if a large number of measurements can be performed. The benefit of this approach is that the separate dataset can be taken independently of the model spectra and the test therefore covers repeatability and helps avoiding overfitting.

3. Experimental

3.1. Instrumentation

Experiments were carried out using an adapted version of an Aryelle 150 spectrometer (LTB, Berlin). This compact spectrograph, which is only 210 mm in its largest dimension, features an Echelle grating which separates the spectral range from 240 to 550 nm into 45 diffraction orders focused after prism cross dispersion on the 2D EMCCD camera Rolera em-c² (Qimaging, Canada). The spectroscopic potential of the Aryelle optical design has been demonstrated already for combined LIBS and Raman investigations using a laser microscope [25] and in a miniaturized version for planetary research applications [26]. The Aryelle 150, which is based on the latter setup, has a focal length of 150 mm and comes up with a spectral resolving power $\lambda/\Delta\lambda_{FWHM}$ of 7500, having a slit width of 50 μm and f/7 aperture, on the small detector area of $8 \times 8 \text{ mm}^2$. The 1004×1002 pixel 14 Bit high speed frame transfer camera is synchronized with the chopper wheel and an external trigger signal created by the conveyor belt. For plasma excitation the double pulse (DP) laser system Twins BSL (Quantel, France) operating at 25 Hz emitting $2 \times 200 \text{ mJ}$ at 1064 nm was used. The laser was focused with a focal length of 800 mm; the beam waist position was located approx. 10 mm above the conveyor belt surface in order to provide the best focus to the majority of samples with the thickness varying between 1 and 30 mm. The first laser pulse was intended to remove paint, dirt or oxide layers whereas the second laser pulse was applied to perform the

actual measurement. An inter-pulse separation of 20 μs was chosen to allow both pulses to overlap on the target moving by 3 m s^{-1} and minimizing interaction between plasmas created by both pulses. The focal length of the collection optics was fixed at 300 mm to have a high tolerance for varying measurement distance as a result of varying sample size. For a schematic of the detection system see Fig. 1. Single burst (one double pulse per sample) measurements were performed allowing the identification and sorting of 25 individual samples per second. The result of the classification is then sent out to a fieldbus system controlling the actual sample separation based on the classification result. The maximum time between sample arrival at the detection system and result arrival at the fieldbus system must not exceed the transit time of 40 ms. The fastest comparable system for single piece identification reported in the literature uses a 40 Hz laser, analyzing the created plasma with a Paschen–Runge spectrometer [4].

The entire system was designed for robustness against physical damage by the samples, strong vibrations in the industrial environment and dust (IP64). Humidity and ambient temperature fluctuation are compensated by housing the components in insulated boxes equipped with active heating and cooling devices keeping every part of the system at its individual optimal operating conditions.

The detection system has no moving parts except for the chopper. Instead, upstream arrangement ensures a constant spacing and positioning of the samples and triggering by a sensor in the final assembly.

3.2. Samples

Samples used in this study were shredded pieces of metals of different elemental composition and of different size and shape taken unaltered from a recycling facility and no further treatment was applied. Sample heights varied between approx. 1 and 30 mm. Most of the samples were covered by a layer of dirt containing significant amounts of calcium. Therefore, most spectra were dominated by the intense emission lines Ca II 393.366 and Ca II 396.845 along with other Ca lines of lower intensity. Classification was performed for nine different alloys with a single main element and one secondary alloy (Ag, Al, Cr, Cu, Fe, Ni, Pb, Sn, Zn and brass) that all needed to be separated from each other. For most classes, at least 100 individual samples were taken to perform model building and validation measurements. For availability reasons, Cr and Sn sample sets contained less samples.

3.3. Data treatment for multivariate classification

Data treatment and calculations were performed using a self-written classification module for the spectrometer software Sophi (LTB, Berlin). Calculations were separated into a training phase and an application phase.

During training, spectra were taken in the lab and models based on them were built and evaluated by validation. As part of the model building appropriate data pretreatment was evaluated and a multivariate model was created and validated using saved data. During optimization of the modeling parameters, pretreatments such as interpolation, spectra rejection by threshold, spectral outlier detection for model building, truncation, normalization, Savitzky–Golay smoothing, binning, differentiation and polynomial baseline correction were tested. Because most pretreatments must not only be applied during model building but also during model application, the time consumption for applying them was equally important as the achieved classification correctness. The pretreatment parameters need to be evaluated for every sorting task and model individually.

The model, containing all information about the required pretreatment and the final chemometrics, was saved as a file and transferred to the sorting facility where it was loaded into the spectrometer software and applied to real time measurements. The benefits of this approach are a high flexibility of the sorting instrument as it can be

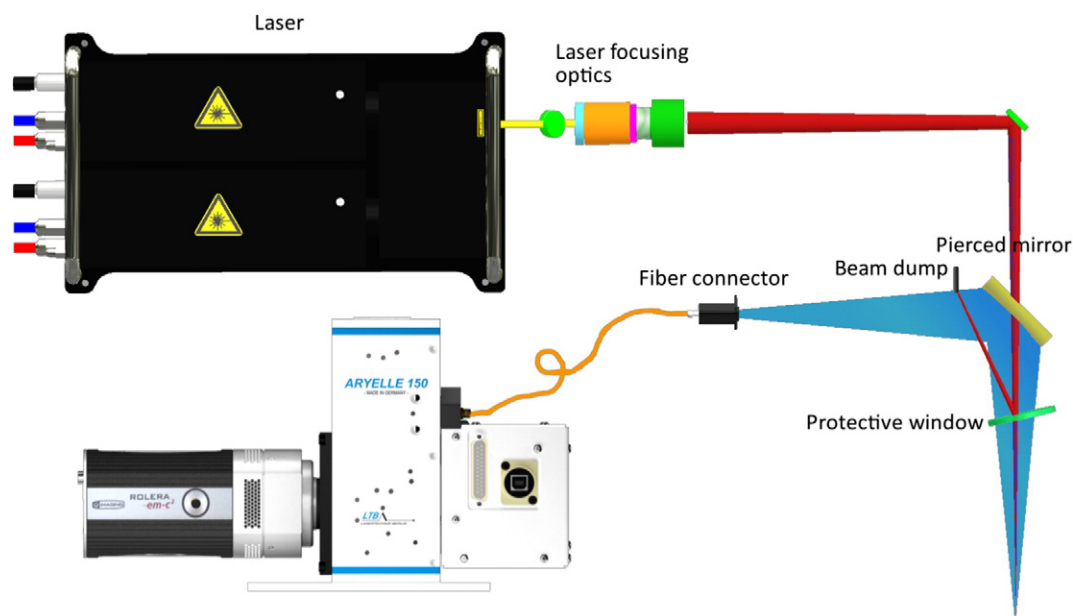


Fig. 1. Schematic of the detection optics used. The laser beam is widened before focusing and then directed through a pierced mirror onto the target. The emitted light from the plasma is collected by a toroidal mirror and focused onto an optical fiber attached to a modified Aryelle 150 spectrometer.

adjusted to new sorting tasks or corrected in case of unpredicted changes in the instrument or ambient conditions.

4. Results and discussion

4.1. Model building

For model building, 100 single burst double pulse spectra for every spectral class were taken. For most classes each spectrum was taken on an individual sample. Only for Cr and Sn repetitive measurements on some samples were necessary.

For PLS-DA analysis, spectra were smoothed, truncated in order to range from 242 to 548 nm and vector normalized. Truncation is done in order to stabilize the system against possible spectral shifts in case of thermal stress. Before normalization, spectra with peak intensity smaller than 750 counts (approx. three times noise) were rejected, because at this level, the spectra are dominated by noise. In the application phase, spectra having such a low maximum intensity will be assigned as class number 0, called trash, to designate that no classification was possible. Number of factors for the PLS-DA was chosen to be number of classes minus one, so in the presented case, the PLS-DA model was calculated for 9 factors. For PCA analysis the spectral pretreatment differs from the PLS-DA pretreatment due to the unsupervised character of the technique. The spectra were as well smoothed and truncated, but additionally, spectral regions dominated by Ca lines originating from the dirt layer on the samples had to be removed to avoid grouping according to the contamination level of the samples. Additionally, the intensity filter for assigning a sample to trash was raised to 1500 counts (approx. six times noise) because at lower values the possibility of misclassifications rose significantly. Finally the spectra were vector normalized. During tests with cross validation, an optimal number of 7 principle components was found and used for the presented work.

For the industrial application, the optimization goal is to have a large percentage of correct classifications (number of true positives versus a number of false negatives) and a low percentage of discarded spectra. Another important measure for the quality of a classification is the purity of the output. It is calculated as the percentage of correctly sorted samples among all samples that were identified to be of the same class (true positives versus false positives). This means, a sample that

cannot be classified correctly should be tagged and removed rather than be grouped with the wrong box thus reducing the purity of that output.

4.2. Validation and testing with saved spectra

To avoid overfitting, validation was always performed with a set of spectra different from the training data. The model was iteratively improved by a stepwise validation approach with increasing complexity of the validation data.

In a first step, validation was performed using a dataset consisting of 1000 spectra of the same samples used for the training data, taken on another day but with the same instrument and experimental parameters. If in this first step a model was found to properly classify the validation set, another, larger validation set containing 8000 spectra taken with the same instrument during several independent measurement campaigns was used. During those measurement campaigns the experimental parameters (inter-pulse delay (8–20 μ s), gate delay (by chopper, 0.3–1 μ s), gain (500–800), binning (1×1 , 2×2), distance of the sample to the fixed focal length optics (± 2 cm)) were varied and tested against the model created with spectra taken with fixed settings. The purpose of this test is to simultaneously check model stability against long time changes in the system and to avoid overfitted models.

Fig. 2 shows the confusion matrices for the classification of the validation data using PLS-DA and PCA as classification models. PCA turned out to show a rather poor classification with the setup used, though preliminary tests using a higher resolution (15,000) spectrometer (Aryelle 400, LTB) for model building and validation showed a good classification power for both PCA and PLS-DA (data not shown). PLS-DA gives a good classification for most alloys. However, silver and brass samples can only be classified with 78 and 71% correct assignments respectively. The most false assignments of silver are copper and brass. This is not surprising because most silver samples were silverware which is usually made of an alloy of silver with copper. Up to 20% copper is not unusual for such samples. Brass is mainly misclassified as copper or zinc. This is also not surprising because both are the main elements forming that alloy. Similar considerations can be made for other misclassifications. Chromium samples from the junk yard are usually chrome plated steel or brass samples. The same applies for nickel samples. Additionally, both types of plating are often combined. This

PLS-DA											PCA														
	Ag	Al	Cr	Cu	Fe	Brass	Ni	Pb	Sn	Zn			Ag	Al	Cr	Cu	Fe	Brass	Ni	Pb	Sn	Zn			
Ag	73	0	0	0	1	0	2	0	0	0	96	Ag	86	25	6	4	5	7	3	5	6	21	51		
Al	3	86	0	2	0	1	0	2	2	2	87	Al	1	63	0	1	0	1	0	1	1	2	90		
Cr	0	0	76	0	0	0	0	0	0	2	97	Cr	0	0	40	0	0	0	0	0	0	1	97		
Cu	9	0	1	83	0	13	1	0	0	0	77	Cu	10	0	2	75	0	38	1	0	0	0	59		
Fe	0	0	3	0	91	2	0	0	1	0	93	Fe	0	6	41	0	89	1	0	0	0	1	64		
Brass	5	0	2	2	0	56	1	0	0	2	82	Brass	0	0	0	9	0	21	1	0	0	1	65		
Ni	0	1	7	0	1	1	82	0	0	1	88	Ni	0	1	6	0	1	1	80	0	0	0	89		
Pb	0	0	1	0	0	0	0	91	1	0	97	Pb	0	0	0	0	0	0	0	85	1	0	98		
Sn	0	0	0	2	0	0	0	0	67	1	95	Sn	0	1	0	3	1	1	0	0	68	1	90		
Zn	3	0	2	0	0	5	4	2	1	72	80	Zn	0	0	0	0	0	1	3	1	0	28	84		
trash	7	13	6	9	4	21	8	5	28	19		trash	3	4	3	6	1	28	10	8	24	44			
% correct	78	98	82	93	97	71	91	95	93	90	89	% correct	88	65	42	81	92	29	90	92	89	50	74		
% trash	7	13	6	9	4	21	8	5	28	19	12	% trash	3	4	3	6	1	28	10	8	24	44	13		

Fig. 2. Confusion matrix for the validation of the PLS-DA and PCA model using a separate set of spectra generated similar to the model spectra using the same samples. Values within the square are the number of classification results for every class. Row trash is the number of discarded spectra for every class, % correct is the percentage of correct results and the average correctness in the right column of that row. The same applies to the % trash row for discarded spectra.

indicates the difficulty for the proper application of a sorting task with real world samples.

Fig. 3 depicts the confusion matrix for PCA and PLS-DA analysis of the aforementioned larger validation set. For the PLS-DA, no significant change in the classification capabilities can be observed. This indicates a good robustness of the model against changes (intentional and unintentional) of the experimental parameters. The PCA on the other hand is affected by a significant drop in the classification capabilities. Correct assignments dropped to values as low as 7% for zinc and 12% for brass. This indicates that the principle components found during model building are not representative for the samples measured but for the measurements themselves. In other words, a serious overfitting has happened that was not detected even with the separate validation set used during model development. This test demonstrates a possible pitfall when building models for the industrial application, where model robustness is of major importance if the sorting machinery is supposed to run 24/7 with as few repeated modeling sequences as possible. Simultaneously, the PCA result presents a good example for the importance of distinguishing between classification correctness and final purity of the sorted samples. While iron samples can be classified with a correctness of 98%, the purity of iron samples in the output is only 28%, due to misclassification of other samples. The vice versa

observation can be made for chromium. While chromium classification is rather poor with 35% correct assignments, the final output is 100% chromium. The same trend exists for zinc. However, if all classes are being identified with a high correctness and remaining errors are mainly random among classes, the purity is also high, which is observable from the confusion matrix of the PLS-DA model.

4.3. Robustness testing

To finally assess the previously created models robustness and versatility, spectra of an extended sample set (for every alloy where more samples were available), including the samples used before, taken with a variety of spectrometers (Aryelle 150, Aryelle 400), cameras (CCD, ICCD and EMCCD) and lasers (Quantel Twins BSL) in different single pulse (SP) and double pulse (DP) configurations (using either one of the laser heads as a SP laser or both as DP) were combined into a data pool containing 11,200 spectra. This is not a use case but only intended to assess the general robustness and flexibility of the chemometric model created with the original setup described earlier. The positive result underlines the general possibility to create models off site with a similar but not the same setup, not interrupting the 24/7 application for taking reference measurements. The classification correctness and

PLS-DA											PCA														
	Ag	Al	Cr	Cu	Fe	Brass	Ni	Pb	Sn	Zn			Ag	Al	Cr	Cu	Fe	Brass	Ni	Pb	Sn	Zn			
Ag	635	1	0	0	0	1	19	4	0	4	95	Ag	678	133	6	43	10	210	49	12	45	355	43		
Al	30	767	1	17	4	28	1	5	7	35	85	Al	4	437	1	1	0	4	0	3	1	7	95		
Cr	0	1	600	0	0	0	4	0	0	3	98	Cr	0	0	240	0	0	0	0	0	0	0	100		
Cu	66	0	4	580	1	67	7	0	0	0	80	Cu	47	0	6	512	1	262	21	0	0	0	60		
Fe	0	5	5	3	618	30	3	2	11	1	91	Fe	78	198	394	47	613	179	100	205	224	139	28		
Brass	6	0	2	10	0	408	10	0	0	2	93	Brass	3	0	1	47	0	94	2	0	0	0	63		
Ni	11	1	33	0	1	1	691	0	0	0	93	Ni	9	1	25	0	1	1	600	0	0	0	94		
Pb	1	0	0	0	0	1	0	725	7	0	98	Pb	1	0	0	0	0	0	0	497	0	0	99		
Sn	0	1	0	2	0	0	3	0	628	1	98	Sn	1	2	0	4	0	2	1	0	415	1	97		
Zn	16	1	2	1	0	35	18	4	2	650	89	Zn	1	1	0	0	0	0	3	0	0	39	88		
trash	96	70	38	108	10	346	51	17	107	136		trash	39	75	12	67	9	165	31	40	77	291			
% correct	83	98	92	94	99	71	91	97	95	93	92	% correct	82	56	35	78	98	12	77	69	60	7	58		
% trash	11	8	5	14	1	37	6	2	14	16	11	% trash	4	8	1	9	1	17	3	5	10	34	9		

Fig. 3. Confusion matrix for the validation of the PLS-DA and PCA model with spectra generated using the same system but varying experimental settings. Values within the square are the number of classification results for every class. Row trash is the number of discarded spectra for every class, % correct is the percentage of correct results and the average correctness in the right column of that row. The same applies to the % trash row for discarded spectra.

PLS-DA													PCA													
	Ag	Al	Cr	Cu	Fe	Brass	Ni	Pb	Sn	Zn			Ag	Al	Cr	Cu	Fe	Brass	Ni	Pb	Sn	Zn				
Ag	931	1	0	0	0	1	24	14	0	4			1049	205	11	87	12	361	68	62	49	624			95	
Al	85	1108	1	45	73	94	3	8	9	154			4	632	1	1	3	5	0	3	1	23			70	
Cr	0	1	637	0	67	0	5	0	0	4			0	0	248	0	8	0	0	0	0	0			89	
Cu	98	0	7	767	1	196	7	0	0	0			58	0	8	687	1	470	26	0	0	0			71	
Fe	1	5	5	14	873	42	4	4	12	5			78	264	430	59	999	205	103	315	265	150			90	
Brass	7	0	5	11	0	708	13	0	0	2			3	0	1	48	0	242	2	0	0	0			94	
Ni	13	1	33	0	1	3	806	0	0	0			11	1	25	0	1	2	706	0	0	0			94	
Pb	2	0	0	1	0	1	1	1046	7	0			1	0	0	0	0	0	1	663	0	0			98	
Sn	0	1	0	12	0	7	3	3	959	1			1	2	0	8	0	3	2	0	705	1			97	
Zn	18	1	4	1	0	44	25	4	2	830			1	1	0	0	0	0	3	0	0	40			89	
trash	105	74	44	120	20	462	59	25	121	180			54	87	12	81	11	270	39	61	90	342				
% correct	80	99	92	90	86	64	90	96	96	83			86	57	34	77	97	18	77	63	69	4	59			
% trash	8	6	5	12	1	29	6	2	10	15			4	7	1	8	1	17	4	5	8	28	8			

Fig. 4. Confusion matrix of the PLS-DA and PCA model validation using spectra generated with different experimental setups and settings. Values within the square are the number of classification results for every class. Row trash is the number of discarded spectra for every class, % correct is the percentage of correct results and the average correctness in the right column of that row. The same applies to the % trash row for discarded spectra.

the purity of the PLS-DA model drops in some cases (e.g. Fe, Zn or brass), however for most classes the classification correctness and purity stay at values larger than 90% (Fig. 4). PCA results are more or less the same as with the larger validation set. The outcome of this test is that the PLS-DA model can be made extremely robust against external influences by carefully selecting appropriate pretreatment algorithms and intense validation.

4.4. Online sorting results

Based on the observations from the previous sections, tests with on-line sorting of fresh untouched samples on site were performed. Samples were manually preclassified and positioned on the conveyor belt in the same way as the machinery does, in a known order to allow the afterward assignment of classification results to the respective samples. Automatic sample positioning would not allow the estimation of the classification correctness but the purity only. Because the conveyor

belt is steel plated, laser pulse misses result in a classification of the samples as iron. Therefore, the classification result iron for other classes is ignored and not treated as an error. The test was repeated four times on two days (two runs per day, Cr, Ni and Pb only once per day) with up to 80 samples per class. The accumulated results are shown in Fig. 5.

Also in this test, the typical misclassifications of brass and silver as copper can be observed. Additionally, an increased amount of rejected results relative to previous tests (average of 18% compared to approx. 10%) is present. This is due to the fresh dirt crust and dust layer on the samples which was already worn down on laboratory test samples. Especially for zinc (39%) and aluminum (24%), a significant increase of trash classifications occurred. This is due to the fact that many samples of those classes are covered with paint which the laser sometimes fails to penetrate with a single burst even with the double pulse laser used. Such samples would require an even stronger cleaning laser or other means of sample cleaning.

5. Conclusion

A versatile system for the simultaneous classification of 10 different types of scrap metal typically found on junk yards by the use of a newly developed high speed Echelle system capable of performing 25 measurements per second was developed. Because single burst measurements are done, this speed translates directly into a sampling speed of 25 samples per second. Classification has been done using PLS-DA showing average classification correctness >88% during online analysis which was shown to greatly excel a PCA based on the same data. The approach presented in this paper is versatile and can be extended to other sample classes by simply changing the model data. This versatility is mainly achieved by the use of an Echelle spectrometer covering a wide spectral range simultaneously at high resolution.

References

- [1] D.W. Hahn, N. Omenetto, Laser-induced breakdown spectroscopy (libs), part ii: review of instrumental and methodological approaches to material analysis and applications to different fields, Appl. Spectrosc. 66 (2012) 347–419 (<http://as.osa.org/abstract.cfm?URI=as-66-4-347>).
- [2] A.K. Myakalwar, S. Sreedhar, I. Barman, N.C. Dingari, S.V. Rao, P.P. Kiran, S.P. Tewari, G.M. Kumar, Laser-induced breakdown spectroscopy-based investigation and classification of pharmaceutical tablets using multivariate chemometric analysis, Talanta 87 (2011) 53–59.
- [3] R. Noll, V. Sturm, Ü. Aydin, D. Eilers, C. Gehlen, M. Höhne, A. Lamott, J. Makowe, J. Vrenegor, Laser-induced breakdown spectroscopy—from research to industry, new frontiers for process control, Spectrochim. Acta Part B 63 (2008) 1159–1166 (A collection of papers presented at the Euro Mediterranean Symposium on Laser Induced

PLS-DA													
	Ag	Al	Cr	Cu	Fe	Brass	Ni	Pb	Sn	Zn			
Ag	220	2	0	0	0	0	0	0	0	2		98	
Al	7	240	2	1	0	6	0	0	0	16		88	
Cr	0	2	70	0	0	1	0	0	0	3		92	
Cu	37	0	3	182	0	51	1	0	0	1		66	
Fe	31	11	34	21	36	34	14	1	7	29		16	
Brass	9	0	4	4	0	228	3	0	0	1		91	
Ni	2	4	5	0	0	1	68	0	0	4		80	
Pb	0	0	1	0	0	5	0	75	2	0		90	
Sn	0	1	0	4	0	3	1	2	87	1		87	
Zn	8	1	1	0	0	4	5	0	0	141		88	
trash	25	85	21	30	2	170	21	2	32	130			
% correct	77	96	81	95	100	76	87	97	97	83		88	
% trash	7	24	14	12	5	33	18	2	25	39		18	

Fig. 5. Online sorting results applying the previously validated PLS-DA model to fresh samples at the sorting facility. Classification result iron is usually due to laser hitting the conveyor belt instead of a sample. Such classification results have been removed in the calculation of the classification correctness. Values within the square are the number of classification results for every class. Row trash is the number of discarded spectra for every class, % correct is the percentage of correct results and the average correctness in the right column of that row. The same applies to the % trash row for discarded spectra.

- Breakdown Spectroscopy (EMSLIBS 2007). <http://www.sciencedirect.com/science/article/pii/S0584854708002504>.
- [4] P. Werheit, C. Fricke-Begemann, M. Gesing, R. Noll, Fast single piece identification with a 3D scanning libs for aluminium cast and wrought alloys recycling, *J. Anal. At. Spectrom.* 26 (2011) 2166–2174.
- [5] D.W. Hahn, N. Omenetto, Laser-induced breakdown spectroscopy (libs), part i: review of basic diagnostics and plasma–particle interactions: still-challenging issues within the analytical plasma community, *Appl. Spectrosc.* 64 (2010) 335A–366A (doi: <http://www.ingentaconnect.com/content/sas/sas/2010/00000064/00000012/art00006>).
- [6] J. Gurell, A. Bengtson, M. Falkenström, B. Hansson, Laser induced breakdown spectroscopy for fast elemental analysis and sorting of metallic scrap pieces using certified reference materials, *Spectrochim. Acta Part B* 74–75 (2012) 46–50 (6th Euro-Mediterranean Symposium on Laser Induced Breakdown Spectroscopy (EMSLIBS 2011)). <http://www.sciencedirect.com/science/article/pii/S0584854712001450>.
- [7] C. Fricke-Begemann, P. Jander, H. Wotruba, M. Gaastra, Laser-based online analysis of minerals, *ZKG Int.* 63 (2010) 65–70 (<http://cat.inist.fr/?aModele=afficheN&cpsidt=24270723> http://www.zkg.de/download/278235/Online_Fricke_Begemann_dt-eng_final_100914.pdf).
- [8] R. Harmon, J. Remus, N. McMillan, C. McManus, L. Collins, J. Gottfried, F. DeLucia, A. Miziolek, Libs analysis of geomaterials: geochemical fingerprinting for the rapid analysis and discrimination of minerals, *Appl. Geochem.* 24 (2009) 1125–1141.
- [9] I. Gaona, J. Serrano, J. Moros, J.J. Laserna, Range-adaptive standoff recognition of explosive fingerprints on solid surfaces using a supervised learning method and laser-induced breakdown spectroscopy, *Anal. Chem.* 86 (2014) 5045–5052.
- [10] X. Zhu, T. Xu, Q. Lin, L. Liang, G. Niu, H. Lai, M. Xu, X. Wang, H. Li, Y. Duan, Advanced statistical analysis of laser-induced breakdown spectroscopy data to discriminate sedimentary rocks based on Czerny–Turner and Echelle spectrometers, *Spectrochim. Acta Part B* 93 (2014) 8–13 (<http://www.sciencedirect.com/science/article/pii/S0584854714000020>).
- [11] J.L. Gottfried, R.S. Harmon, F. C. D. Jr., A.W. Miziolek, Multivariate analysis of laser-induced breakdown spectroscopy chemical signatures for geomaterial classification, *Spectrochim. Acta Part B* 64 (2009) 1009–1019.
- [12] C. Jirang, H.J. Roven, Recycling of automotive aluminum, *Trans. Nonferrous Metals Soc. China* 20 (2010) 2057–2063.
- [13] R. Noll, C. Fricke-Begemann, M. Brunk, S. Connemann, C. Meinhardt, M. Scharun, V. Sturm, J. Makowe, C. Gehlen, Laser-induced breakdown spectroscopy expands into industrial applications, *Spectrochim. Acta Part B* 93 (2014) 41–51 (<http://www.sciencedirect.com/science/article/pii/S0584854714000160>).
- [14] N. Savage, Scientific ccd cameras, *Nat. Photonics* 1 (2007) 351–353 (<http://dx.doi.org/10.1038/nphoton.2007.91>).
- [15] M. Mueller, I.B. Gornushkin, S. Florek, D. Mory, U. Panne, Approach to detection in laser-induced breakdown spectroscopy, *Anal. Chem.* 79 (2007) 4419–4426 (pMID: 17503765).
- [16] H. Heilbrunner, N. Huber, H. Wolfmeir, E. Arenholz, J. Pedarnig, J. Heitz, Comparison of gated and non-gated detectors for double-pulse laser induced plasma analysis of trace elements in iron oxide, *Spectrochim. Acta Part B* 74–75 (2012) 51–56 (6th Euro-Mediterranean Symposium on Laser Induced Breakdown Spectroscopy (EMSLIBS 2011)). <http://www.sciencedirect.com/science/article/pii/S0584854712001437>.
- [17] J.B. Sirven, B. Bousquet, L. Canioni, L. Sarger, S. Tellier, M. Potin-Gautier, I.L. Hecho, Qualitative and quantitative investigation of chromium-polluted soils by laser-induced breakdown spectroscopy combined with neural networks analysis, *Anal. Bioanal. Chem.* 385 (2006) 256–262.
- [18] S.R. Goode, S.L. Morgan, R. Hoskins, A. Oxsher, Identifying alloys by laser-induced breakdown spectroscopy with a time-resolved high resolution Echelle spectrometer, *J. Anal. At. Spectrom.* 15 (2000) 1133–1138 (<http://dx.doi.org/10.1039/B002190N>).
- [19] H. Fink, U. Panne, R. Niessner, Process analysis of recycled thermoplasts from consumer electronics by laser-induced plasma spectroscopy, *Anal. Chem.* 74 (2002) 4334–4342 (pMID: 12236340. <http://dx.doi.org/10.1021/ac025650v>).
- [20] P.R. Peres-Neto, D.A. Jackson, K.M. Somers, Giving meaningful interpretation to ordination axes: assessing loading significance in principal component analysis, *Ecology* 84 (2003) 2347–2363.
- [21] W. Kessler, *Multivariate Datenanalyse für die Pharma-, Bio-, und Prozessanalytik*, Wiley-VCH, Weinheim, 2007.
- [22] P. Geladi, B.R. Kowalski, Partial least-squares regression: a tutorial, *Anal. Chim. Acta* 185 (1986) 1–17 (<http://www.sciencedirect.com/science/article/pii/0003267086800289>).
- [23] C. Beleites, R. Salzer, Assessing and improving the stability of chemometric models in small sample size situations, *Anal. Bioanal. Chem.* 390 (2008) 1261–1271.
- [24] M. Pontes, J. Cortez, R. Galvão, C. Pasquini, M. Araújo, R. Coelho, M. Chiba, M. Abreu, B. Madari, Classification of Brazilian soils by using libs and variable selection in the wavelet domain, *Anal. Chim. Acta* 642 (2009) 12–18.
- [25] M. Hoehse, D. Mory, S. Florek, F. Weritz, I. Gornushkin, U. Panne, A combined laser-induced breakdown and Raman spectroscopy Echelle system for elemental and molecular microanalysis, *Spectrochim. Acta Part B* 64 (2009) 1219–1227 (DOI: <http://www.sciencedirect.com/science/article/B6THN-4XBR4MB-1/2/18062a18f5694359e60cf8416d751b0a>).
- [26] S. Pavlov, E. Jessberger, H.-W. Hübers, S. Schröder, I. Rauschenbach, S. Florek, J. Neumann, H. Henkel, S. Klinkner, Miniaturized laser-induced plasma spectrometry for planetary in situ analysis—the case for Jupiter's moon Europa, *Adv. Space Res.* 48 (2011) 764–778 (europa Lander: Science Goals and Implementation. <http://www.sciencedirect.com/science/article/pii/S0273117710004527>).